Anisotropic Hardware Injection of Gravitational Waves into LIGO Detectors

A THESIS
SUBMITTED TO THE FACULTY OF THE GRADUATE SCHOOL
OF THE UNIVERSITY OF MINNESOTA
BY

Miranda Pihlaja

IN PARTIAL FULFILLMENT OF THE REQUIREMENTS
FOR THE DEGREE OF
MASTER OF SCIENCE

Dr. Vuk Mandic

August 2011

Copyright

Miranda Pihlaja, 2011 ©

Acknowledgements

LIGO has been a huge part of my scientific and professional development. I can honestly say it was because of the opportunities I was given at LIGO that I got into graduate school for physics. From being a normal citizen on the public tour in 2006 to a teacher with the I2U2 program to a teacher intern to a Master's student, I've had the privilege of interacting with LIGO on many different levels. I have always appreciated how open and generous the people at LIGO are with their work and their time. They have a keen understanding that training people takes patience, time, and a lot of conversation. Thank you to the staff at LIGO including but not limited Dale Ingram, Mike Landry, Fred Raab, Dick Gustafson, Greg Mendell, and Cheryl Vorvick for the many lunch talks, the numerous hours explaining the details of the instrument, and the insight into what having a science career entails.

As this project got underway, these kind souls were very helpful in details of how to find files on the LIGO computers, C++ and MatLab coding, and in helping me understand what I was doing and giving me a voice in LIGO. I would like to include a thank you to Eric Thrane for fielding hundreds of questions along the way especially in the early parts of the project and to Shivaraj Kandhasamy for the many conversations about what's really happening in the instrument and for the editing help with this paper.

I have been so grateful to have Vuk Mandic as my advisor for this project. He is a patient teacher, a conscientious advisor, an amazing editor, and all around nice person. I appreciate that he gave me a project that was much too big for me and guided me through it without making it a miserable experience. I realize that this is a unique gift.

And finally, I must say thank you to my family and friends who have patiently listened to my explanation of gravitational waves and have been so encouraging through the bruises of graduate school in the last three years. Don't worry, my next project is much easier to understand. I would also like to say a special thank you to Dan Endean who read my thesis draft, let me see into the mind of my audience and gave me so many helpful editing suggestions.

Abstract

The goal of LIGO (Laser Interferometer Gravitational-wave Observatory) is to measure very small changes in the length of its arms caused by gravitational waves stretching and compressing space-time. The purpose of this project was to perform a search pipeline test on the LIGO detector using a point source stochastic signal. Here we report an effort to test the LIGO stochastic data-analysis pipeline using a simulated hardware injection. A hardware injection is an end-to-end test that begins with the generation of a signal and ends with the recovery of the signal from the detector's strain data. The signal is injected into the interferometers by actuating on a test mass (or mirror) in order to shake it to simulate a gravitational wave. We successfully recovered the hardware injection with measured parameters consistent with injected parameters, thus providing an end-to-end test of the stochastic data-analysis pipeline.

Table of Contents

List of Figures

Chapter 1: Gravitational Wave Background

I. Background and theoretical motivation

For millennia, scientists have been tracking the movement of the cosmos to try to unlock its mysteries. The main way to probe the history of the universe thus far has been to detect the electromagnetic signals such as visible light, gamma radiation, or X-rays. If these signals can be thought of as the 'sights' of the universe, gravitational waves are the 'sounds', which carry another set of information from cosmic activity. The detection of gravitational waves would allow us to both have experimental confirmation of the theory of relativity and have another way to observe astrophysical and cosmological phenomena.

Gravity is thought of as the stretching of space-time and is described by Einstein's theory of relativity. Gravitational waves are a consequence of this theory. It can be shown that in the weak-field limit the perturbation of space-time, $h_{\mu\nu}$, obeys the relationship:

$$(\nabla^2 - \frac{1}{c^2}\frac{\partial^2}{\partial t^2})h_{\mu\nu} = 0$$

where c is the speed of light, which then shows that the space-time metric has wave-like behavior with a propagation velocity equal to the speed of light.

To date, the distortion of space-time has been observed by how it affects surrounding masses, photons, and other particles traveling through space-time. Gravitational waves have not yet been directly detected experimentally, but the use of interferometry is pushing the bounds of our current range of observation. The question now is less about if we can detect these signals but when we will see them. Direct detection of gravitational waves can provide information about the events of the early universe, mergers of neutron stars and/or black holes, or dynamic processes in neutron

stars that cannot be detected otherwise. This project deals with the operation of the detectors called LIGO (Laser Interferometer Gravitational-wave Observatory) by testing whole process of modeling a gravitational wave source, physically simulating the signal on the detectors and recovering it from the data acquired by the detector.

II. Sources

This section will discuss what is necessary for a gravitational wave to be produced and what some of the sources of these waves are. According to general relativity, a gravitational wave is produced by an acceleration of a mass with a quadrupole moment or higher. While a simple wave of a hand meets these criteria, due to the stiffness of the space-time metric only colossal events such as a collision between stars will potentially release enough energy to generate an observable gravitational wave. The gravitational waves caused by these events have been undetectable with instruments in the current ranges of sensitivity.

Observable gravitational waves are produced by two main sources: cosmological and astrophysical. Two of the goals of detecting gravitational waves are to probe the unresolved events of the early universe and to be able to detect the signals that astrophysical sources generate. The cosmological sources happened around the time of inflation, and the signals still propagate throughout the universe. The astrophysical sources come from more 'recent' events in the universe involving large structures such as stars or black holes. The largest gravitational waves will be produced by astrophysical events that may be observed in other ways such as visible light from a supernova or gamma radiation bursts; however, the nature of cosmological events around the time of

inflation is largely unknown and must be constructed from the information that is yet to be measured.

Although the idea of gravitational waves was postulated by Einstein in 1916, it was not until decades later that the first indirect evidence of these waves was observed from an astrophysical source. Gravitational waves were found to correctly describe the energy loss of the binary pulsar system PSR 1913+16 [1]. The frequency of the binary system has been decreasing at the rate predicted by general relativity via gravitational waves to within 0.3% [2]. The system was discovered by Hulse and Taylor in 1974 resulting in the Nobel Prize in 1993 [2][3].

Other astrophysical sources include inspiraling binary systems and supernovae. Inspiraling binary systems have an increase in angular frequency as the two objects spin into each other and collide or coalesce releasing a massive amount of energy. Binary systems can be comprised of black holes, neutron stars or a combination of the two. Supernovae will also release massive amounts of energy during the core collapse that can be carried away in neutrinos and photons or as gravitational wave signals. Since supernovae can be observed using electromagnetic radiation, there could be another confirmation of the event, where it took place and how much energy was released. Astrophysical sources give the most promise for the first detection of gravitational waves.

There are numerous theories surrounding the epoch of inflation and the cosmological events that occurred around that time. One example of how gravitational waves could have been involved in the early universe is during big bang nucleosynthesis or BBN. As the universe expanded after inflation, BBN was the epoch of forming helium and other light elements. The presence of gravitational waves before and during BBN

could have altered the rate of expansion of the universe, and therefore have affected the amounts of lightest nuclei formed. The number of relativistic particle species at the time of BBN has been determined to be $3.08 + 0.74 / -0.68$ by observations of helium abundance in the universe [4]. This number is consistent with the three types of relativistic particles called neutrinos that have been confirmed experimentally, however the uncertainty in the number leaves room for relativistic contributions from gravitational waves created before BBN. Since there is uncertainty surrounding the occurrence of inflationary events, the signals from these events cannot be modeled exactly. The detection of signals from the early universe will give insight into the physics of highest energy scales that determined the behavior of the universe in the epoch.

Chapter 2: Detection and Search groups

I. Detectors

Joseph Weber constructed the first gravitational wave detector in the 1960's [2]. The bar detector was made of aluminum with a piezoelectric diode fixed to one end to measure the lengthening and contracting of the bar when a gravitational wave propagated through it. While what now is known about the sensitivity needed to detect gravitational waves makes this early effort seem futile, it was the first step in attempting to measure the presumably un-measurable signal. Although the bar detectors have not been completely abandoned, the development of interferometry opened the ability to measure length scales in the range of a perturbation due to gravitational wave signals.

The interferometer will measure the gravitational wave by measuring its differential arm length called strain (h), which is defined as

$$h = \frac{\Delta L}{L}$$

where L is the length of the interferometer arm and ΔL is the change in the arm length. The current instruments can measure strains on the order of 10^{-22} [5]. The ground based Michelson interferometers are able to detect changes in the length of the arms of $10^{-18} - 10^{-19}\, m/\sqrt{Hz}$ in the 40Hz to several kHz range [6].

Another unit of measure of the gravitational wave is energy density defined as

$$\Omega_{GW}(f) = \frac{f}{\rho_c}\frac{d\rho_{GW}}{df}$$

where $d\rho_{GW}$ is the energy density of the gravitational radiation in a small frequency range df, ρ_c is the critical energy density of the universe, and f is frequency [7]. The stochastic gravitational wave background is produced by an incoherent superposition of unresolved sources. The energy density of gravitational waves generally applies to stationary signals, and stochastic sources are usually assumed to be stationary. Stochastic signals can be produced by either cosmological or astrophysical sources. Searching for these sources involves looking for power distributions in the sky and then integrating it to determine the energy density. The energy density of various sources is shown in figure 1. Recent results from LIGO show that the upper bound of energy density for stationary waves is

$$\Omega_{GW} < 6.9 \times 10^{-6}$$

in the 51-150 Hz frequency range [7]. This bound puts the instrument potentially in the range of being able to detect gravitational waves from some cosmological and stationary astrophysical sources (see figure 1)

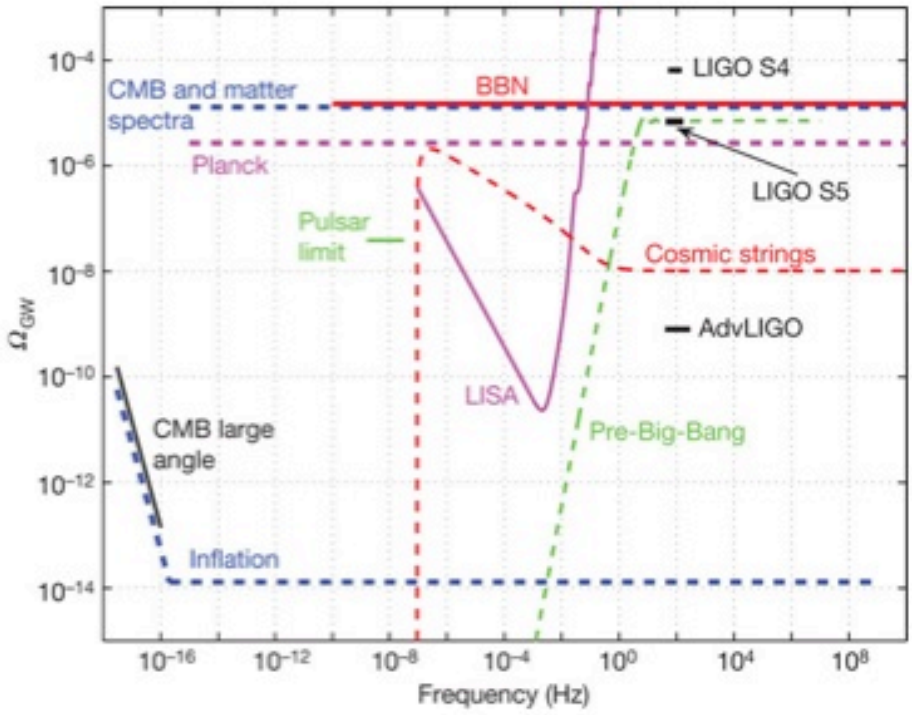

Figure 1: This graph is a landscape of the energy densities of various cosmological and astrophysical gravitational wave models compared to several experiments and observations. Advanced LIGO (AdvLIGO) is scheduled to begin its run in 2014 [7].

II. Gravitational Wave Groups

Each gravitational wave has a specific signal or signature that identifies the source from which it originated. The LIGO Scientific Collaboration has groups that are looking for signals from specific sources including pulsars, inspiraling systems, and stochastic sources. Each group combs through the data searching for signals expected from the respective sources. There are two ways that we test our ability to recover theoretical signals from the data of the detectors. The first is a software injection, which inserts the simulated signal into the output data from the detector. This primarily tests the recovery algorithm's effectiveness at retrieving signals from the output data. The second test is a hardware injection, which takes the theoretical signal and physically puts it onto the

detector by moving the interferometer mirrors so that the signal is in the final data collected. This is done to test the response of the detector to a physical signal.

We will model a theoretical source with its sky map of strain power. A sky map is a distribution of some quantity such as power on the celestial coordinate system. Declination and right ascension are earth-based celestial coordinates where zero degrees corresponds to the equatorial plane of the earth and zero hours is the time when the sun crosses the equatorial plane during vernal equinox. The sky map in figure 2 is a power distribution of a point source signal at a right ascension of 6 hours and declination 45 degrees with a strain power $3.2\times10^{-45}\ strain^2 / Hz / rad^2$.

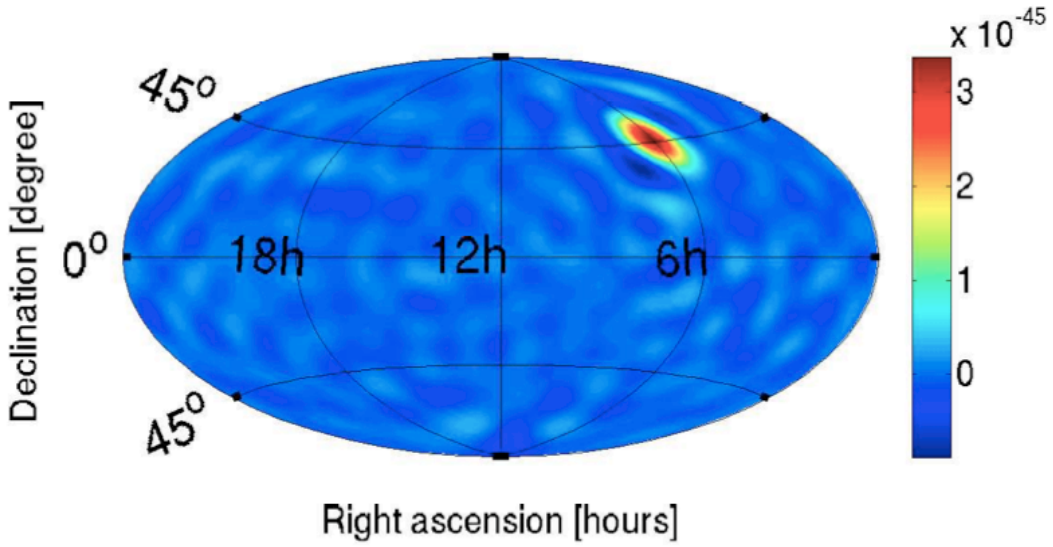

Figure 2: Sky map shows the power distribution of a point source at 6 hours, 45 degrees. The highest power is about 3.2e-45 $strain^2 / Hz / rad^2$ **[8]**

A gravitational wave signal can be decomposed into a linear combination of spherical harmonic vectors (Y_{lm}) that make up the power distribution $P(\Omega)$ given by

$$P(\Omega) = \sum P_{lm} Y_{lm}$$

where *l* and *m* specify the resolution of the signal's location. Each Y_{lm} has a coefficient

(P_{lm}) that scales each Y_{lm} 's contribution to the overall signal [8].

The Stochastic group at the University of Minnesota is searching for signals from unresolved sources. The sky maps for these sources only represent theoretical power distributions. A few examples of what could produce stochastic signals are a stochastic point source, multiple point sources in different locations, and an extended power distribution across the sky, which could be isotropic. Figures 2-6 are sky maps of various anisotropic stochastic sources. While each of these signals has a specific source distribution, the group looking for stochastic sources would like to be able to identify any gravitational wave signal in the data without knowing a priori what is its distribution.

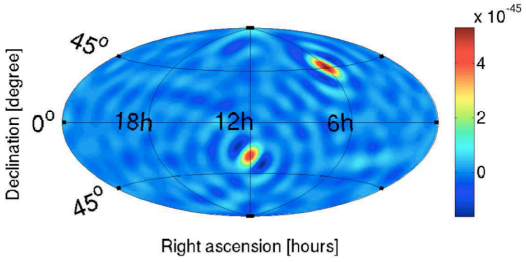

Figure 3: Two point sources [8]

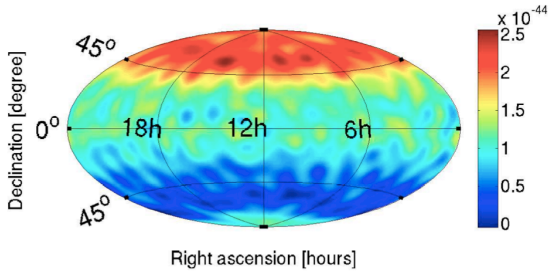

Figure 4: Dipole source [8]

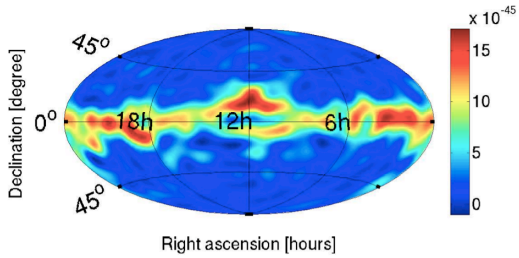

Figure 5: Diffuse source at zero degrees [8]

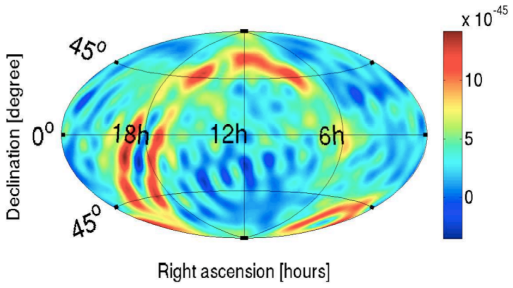

Figure 6: Diffuse source in the galactic plane [8]

III. LIGO

LIGO employs twin Michelson interferometer whose schematic diagram is seen in figure 7.

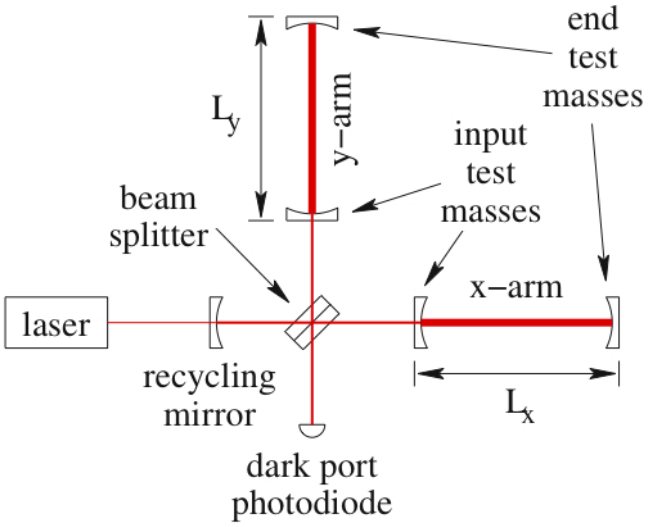

Figure 7: Schematic diagram of the LIGO interferometer [9]. The instrument has arm lengths of 4km. The arms are calibrated to produce completely destructive interference on the dark port photodiode unless there is stretching or compressing due to a gravitational wave.

The approximately 10-Watt laser beam passes through the beam splitter and travels down either one of the 4-kilometer Fabry-Perot cavity (Lx, Ly) and is reflected in the respective cavities on average one hundred and fifty times before being combined again. The multiple trips of the light in the arm of the interferometer increase the sensitivity of the instrument. Any perturbation of the arm length by a gravitational wave will increase the phase shift of the light by the number of trips in the arm. This will phase shift the combined light to create constructive interference on the photodiode detector. The intensity of the light observed on the photodiode and the pattern of interference is dependent on the amplitude and polarization of the gravitational wave. The end test masses or mirrors are suspended by wires, which makes them behave like pendulums. They have magnets attached to the faces, which allow control of their movement using electromagnets. There is a feedback loop from the dark port photodiode to the electromagnets controlling the mirrors in order to keep the mirrors still. The hardware injection puts the signal into this feedback loop to introduce the simulated signal on one of the mirrors.

LIGO incorporates fraternal twin detectors located in Hanford, WA and Livingston, LA, which are about 3,000 miles apart. Having two detectors in different locations with different orientations provides the data needed to confirm that signal was detected. If the signal is stationary, as is the case with anisotropic stochastic signals that we will investigate here, the location of the source can be determined using the lag time of the signal's arrival between the two detectors and the rotation of the earth which breaks the degeneracy of the location. There is a band of locations in the sky that would

give the same lag time between the detectors so the information from the rotation of the earth will pinpoint the source's location.

The isolation of the instrument is important since almost everything in the environment that creates a background noise is louder than the gravitational wave signal. Having twin detectors gives the ability to reject the noise of the local environment such as seismic activity and electromagnetic fluctuations. LIGO collaborates with other Gravitational-Wave detectors around the world including VIRGO (Italy), GEO (Germany), and TAMA (Japan), though VIRGO is the only other interferometer in the same range of high sensitivity.

Chapter 3: Project and Code Modification

I. Pipeline test

The pipeline test ensures that the detector responds to particular signals as expected and checks that every point in the process is working properly. It is necessary to perform these checks in order to be confident that the signals are recovered reliably. Software injections can be done at any time because the signals are put into the data from the instrument after it has been collected. There is no interference with the instrument's operation thus they do not affect the sensitivity. Hardware injections, on the other hand, are physical signals artificially generated on the mirrors of the interferometer, therefore they compromise the sensitivity of the interferometer and usable data. Hardware injections are run much less frequently by each of the search groups but they are necessary as a confirmation for potential detections. The instrument's response to known signals must be well understood in order to claim there is a candidate detection for a gravitational wave.

This project is a pipeline test of the anisotropic stochastic single point source signal similar to the one in figure 2 and is the only hardware injection of an anisotropic stochastic signal to date. It starts by generating the signal used in the software injection for the point source, modifies the signal waveform so that it can be applied to the detector mirrors, and recovers the signal from the detector's output.

The software injections code, which was developed by the LIGO Stochastic Working Group, calculates each of the spherical harmonic coefficients (P_{lm}) based on the strength and location of the signal and the rotation of the earth. The code outputs a time series signal, which is an amplitude of strain in time sequential order. A Fourier Transfer was applied to the data to convert it into a frequency series in order to apply a pendulum transfer function to the data. The mirrors at the ends of the arms of the detector are suspended by very fine wires and behave like pendulums. When the mirror is driven at various frequencies, it will respond differently to each frequency. In particular, the pendulum's response to the driving force goes as $\left(\frac{1}{frequency^2}\right)$ for frequencies above the resonant frequency of the pendulum. In order to generate a constant strain on the mirror across all frequencies, we must scale the injection signal with the inverse of the pendulum's response (i.e. with $frequency^2$ times the appropriate calibration factor). After applying the transfer function, an inverse Fourier transform was applied to the data to convert it back to a time series and written to a text file.

In order to pass the data on to the interferometer, we modified the existing hardware injection program to read in the text files, converted the signal in binary format, and passed it to the Arbitrary Waveform Generator (AWG). AWG represents the

interface with the LIGO front-end system, which converts digital signals into analog currents that then drive the interferometer mirrors. The signal is injected into the feedback loop between the dark port photodiode, or DARM_ERR, and the mirrors.

Details that needed to be addressed were the amount of data being generated at any one time and the continuity of the signal being passed to the instrument. The injection was intended to last for a continuous 24-hour period in order to have the best resolution of the point source in the sky. Each 60-second text file was on the order of 1 GB large, which would have generated about 1 TB of data for the whole injection. This made generating all of the data prior to performing the injection impractical. It was decided that the software injection code that generated the time series data would be run interactively on MatLab producing three 60-second files in the directory at a time. The hardware injection code was run in parallel, reading in each data file one at a time and deleting them after they were injected. In order to ensure that the data was continuous at the ends and beginnings of each of the text files, an overlapping time series was generated and each segment was windowed using a sine function so that every text file matched up with no breaks in the signal.

II. Code Modification

The following paragraph addresses the details of the programming codes used and how they were modified in this project. Figure 8 is a flowchart of the codes interaction and modifications.

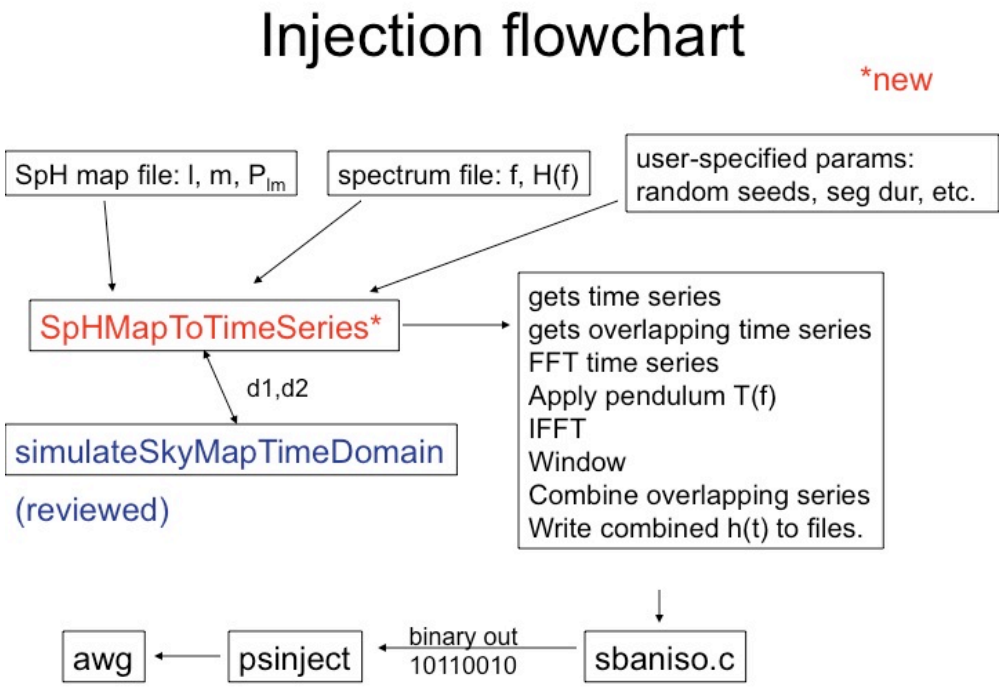

Figure 8: Flowchart of the hardware injection process [14].

The two main codes used for this injection both have been reviewed by the LIGO collaboration and used in either software or hardware injections. The first code is sb.c, which generates a time series for an isotropic injection and passes the data in binary format on to AWG. This code was modified by V. Mandic to only read in the text files with the injection data and renamed sbaniso.c. The code for the anisotropic software injection is called simulateSkyMapTimeDomain.m and was written by J. Romano and S. Balmer. The spherical harmonic coefficients are calculated by a routine in the code, and the user sets parameters of frequency spectrum, start time, random seed, location and injection duration. A parent routine, SphMapToTimeSeries.m, loads the user parameters and calls simulateSkyMapTimeDomain.m, which returns time series and overlapping time series for the LIGO Hanford and LIGO Livingston detectors.

Since the time series were generated in one-minute segments and written to separate text files, the overlapping time series was generated to provide continuity of the signal between the files. The overlapping series was a 60-second segment of the signal offset by 30 seconds. Both the original time series and the overlapping time series 60-second segments were multiplied by a sine function, which reduced the amplitudes of the beginning and the end of the segment to zero and maximized the amplitude in the middle (see figure 9).

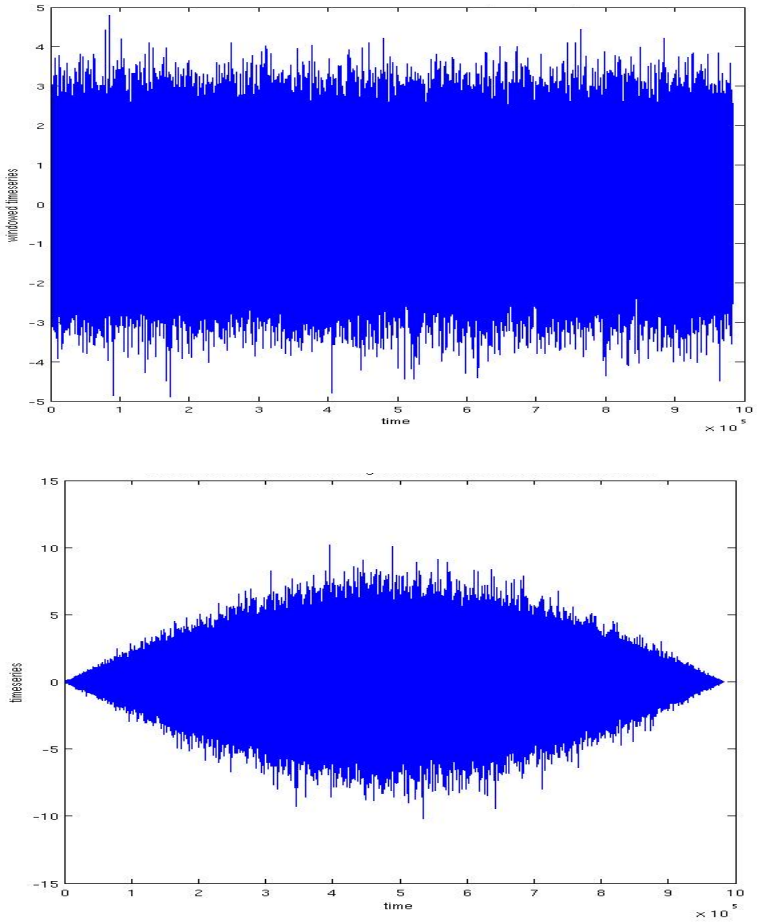

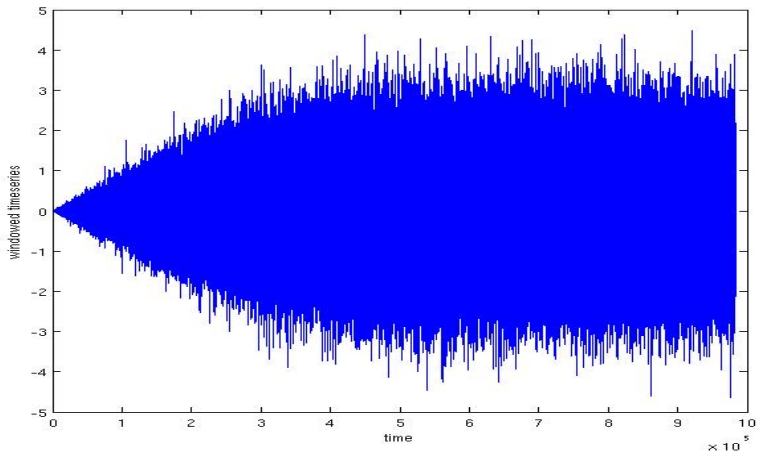

Figure 9: Windowing and overlapping series. This graph shows three different 60-second time series segments in the windowing and combining process. These are only examples of the overlap-combining process. The first panel shows the original time series. The second panel shows the time series after it has been windowed by half of a sine function. The third panel shows the first 60-second combination of the overlap time series and the original time series. The x-axis corresponds to time on the order of microseconds as the sampling frequency is on the order of 16,000 Hz.

The overlapping time series was cut into two parts with the first half being added to the end of the first time series segment and the second half being added to the first part of the next time series segment. This ensured that the signal had a constant amplitude throughout each segment and that the end and beginning of each time series segment was continuous.

The modifications to the time series in SphMapToTimeSeries.m for the hardware injection are as follows:

- Fourier transfer both time series to the frequency spectrum
- Apply pendulum transfer function (tfH) to the frequency series as defined in sb.c[1]
  - $tfH = \dfrac{frequency^2}{(2.05e-13)(0.764Hz)(0.764Hz)}$
  - resonant frequency of the pendulum = 0.764 Hz

[1] This transfer function is specified for only the Hanford detector. The Livingston detector has a different calibration constant and resonant frequency.

- 2.05*e*-13 calibration constant at Hanford
- inverse Fourier transfer back to a time series
- Window time series using sine function
- Combine time series and overlapping time series
- Write to text files

Since the injection was intended to be run for one day, the amount of data that was being processed at any given time was limited to three text files by having the program check for three files in the folder before generating the next minute and deleting each file after it was used. The SphMapToTimeSeries.m code was interactively run on Matlab and the text files were saved in the same directory on the server. The text files were then read in by sbaniso.c, which converted the data to binary and passed it to AWG.

Chapter 4: Analysis and Recovery

I. Expected signal

The point source signal was injected at a location of 6 hours and 45 degrees in the same location as the signal in figure 2. The strain amplitude was constant across a frequency spectrum of 1/60 to 1800 Hz. The intended injection power was 1.6e-45 $strain^2 / Hz / rad^2$. This signal location and power magnitude had previously been used in a software injection. One source of uncertainty in the instrument that can be mostly accounted for is the calibration of the pendulum transfer function. The pendulum transfer function used in the code modification is the expected response of the mirrors to being driven at various frequencies. The actual pendulum response of the instrument is measured at various times throughout the scientific runs at LIGO. While these

measurements do not give the exact factor difference for the whole run, they are used to rescale the expected power magnitude of the injected signals.

The equation to rescale the expected power magnitude of the signal is as follows

$$P'_{theo} = \left(\frac{M_{H1}}{E_{H1}}\right)\left(\frac{M_{L1}}{E_{H1}}\right)P_{theo}$$

where M_{H1} and M_{L1} are the measured pendulum transfer calibrations of the Hanford and Livingston LIGO detectors and *E* is the expected pendulum transfer function that was used to generate the injection signal from the strain[2]. While these transfer functions depend on frequency, the ratio between the measured and expected functions will remain constant. The rescaled expected power magnitude is

$$P'_{theo} = (0.58)P_{theo} = 0.92 \times 10^{-45} strain^2 / Hz / rad^2$$

The inspiral range of LIGO is a figure of merit describing LIGO sensitivity- it is the distance (in megaparsecs) at which LIGO would be able to detect a binary neutron star inspiral (of 1.4 solar masses each). The target inspiral range for LHO and LLO is between 15 and 20 megaparsecs (Mpc), and both interferometers need to be in this range, in what is called coincidence, for the data to be usable and have appropriate sensitivity for recovery. Several reasons why the instruments may not be functioning at sensitivity are local seismic activity from either human or geophysical sources, windstorms, or local electromagnetic fluctuations. Even though the injection was intended to run for 24 hours, there were two separate injections run due to low sensitivity in the instruments the first day and a malfunction of the first injection after running for 1000 minutes. The first injection was run on July 20-21, 2010 at LIGO Hanford Observatory and LIGO

[2] Note: The same expected pendulum transfer function was used for both Hanford and Livingston

Livingston Observatory starting at 13:30 (UTC time). Figure 10 shows that there was no time in the Inspiral Range graph on July 20th that both instruments were functioning at an acceptable sensitivity after the injection started at -4 hours. Figure 11 shows the measured strain power in several frequency bands. The highest frequency sensitivity of LIGO is in the 100-200 Hz band, which is seen as a green line in the Hanford graph and a blue line in the Livingston plot. Ideally, the band has a lower power, which means the detector is more sensitive to increases of power due to a gravitational wave signal in that frequency band. The hardware injection's effect on the detector's strain power recovery can be clearly seen in the DARM_ERR graph in figure 12 at -3.5 hours. The green line drops down which indicates smaller amount of power in that band when the first injection is turned off. Similarly in figure 14, there is a drop in the 100-200 Hz band at -8.5 hours and gain at -7.5 hours corresponding to when the injection is started and stopped. This effect is not as pronounced in the Livingston instrument's power as seen in figures 13 and 15.

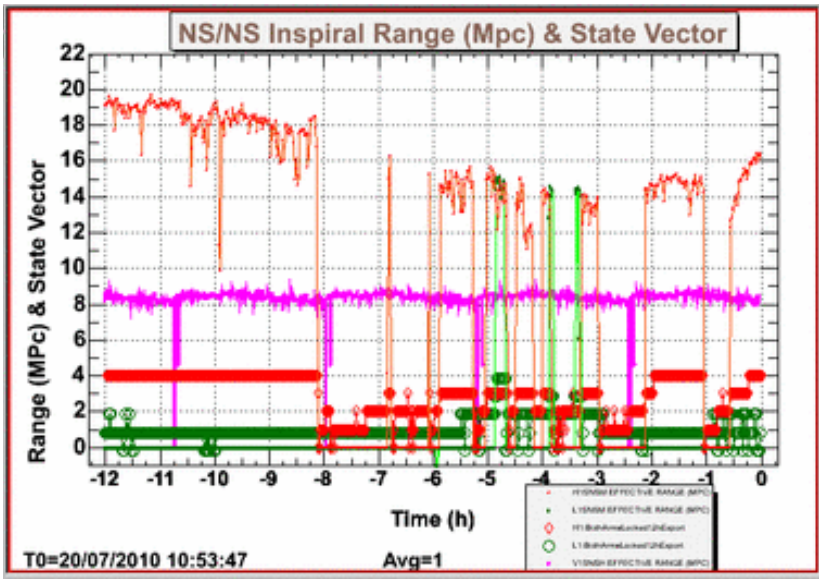

Figure 10: Inspiral range plot: first injection, first day. This graph shows the inspiral range sensitivity of the Hanford (red line) and Livingston (green line) interferometers. During this time

frame, the Hanford interferometer had about 4 hours of acceptable sensitivity from -12 to -8 hours and sporadic sensitivity for the rest of the time frame. The Livingston interferometer had almost no time within the sensitivity range needed for usable data. Injection started around -4 hours (06:34, 20/07/2010). The State vectors (the red and green bars) show four different levels of functionality of the instruments. At beginning of the graph, Hanford (red bar) is at full functionality and Livingston (green bar) is at lowest functionality.

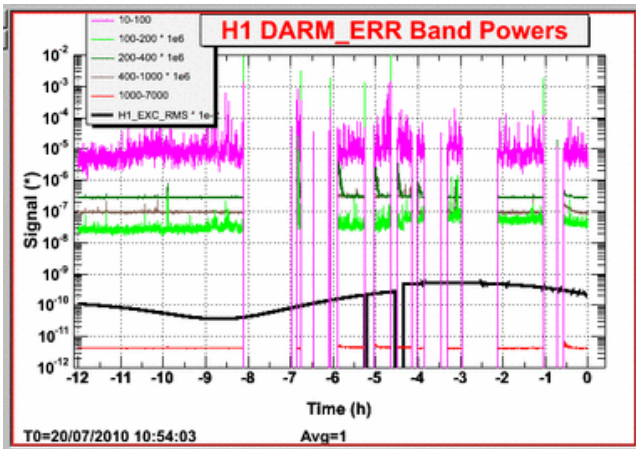

Figure 11: Power measured at WA LIGO: first injection, first day. This graph shows the recovered power in different frequency bands. The main frequency band for this injection is the 100-200Hz. When the injection is driving the mirrors, the power in that frequency band is larger, which is undesirable. A lower strain power in any frequency band allows the interferometer to detect smaller changes from gravitational waves.

Figure 12 shows the sensitivity of the instrument was acceptable in the last two hours of the injection on July 21, 2010 between the hours of -6.5 and -4.5 on the graph.

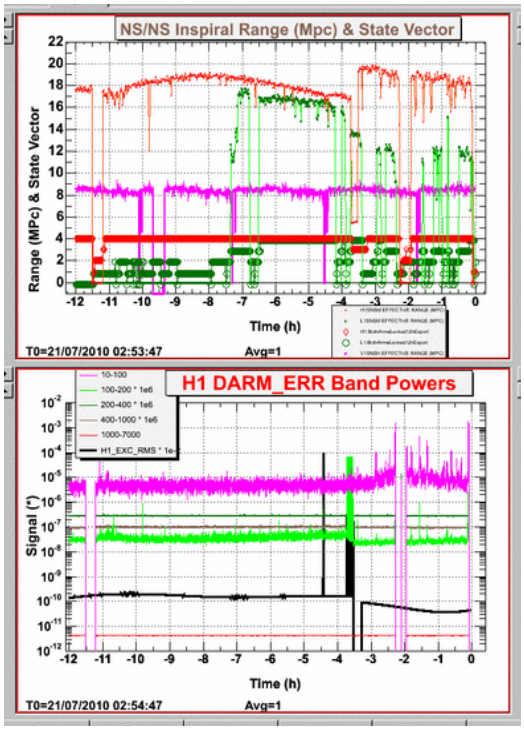

Figure 12: Inspiral range: first injection, second day. The instruments were in the acceptable range of sensitivity and in coincidence between around -6.5 and -4.5 hours. Injection was stopped around -3.5 hours (23:34, 20/07/2010) due program malfunctioning. The strain sensitivity in the 100-200Hz band increased when the injection was turned off. See captions for figures 11 and 12 for description of plots.

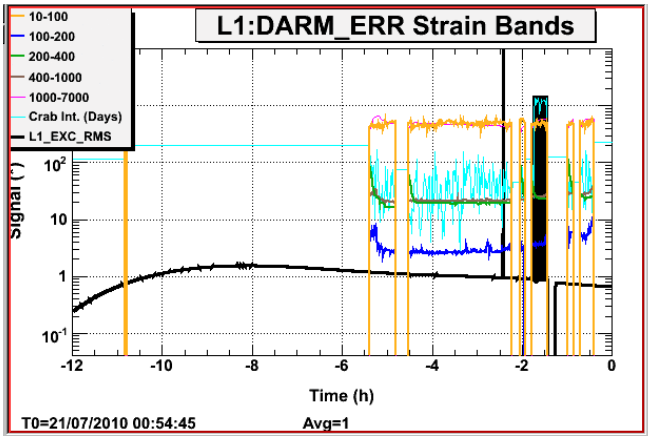

Figure 13: Power measured at LA LIGO: first injection, second day. The usable injection data was between -4.5 and -2.5 hours and the injection was turned off just before -1.5 hours due to a malfunctioning of the injection.

The second injection was run on July 25, 2010 starting at 14:30 and ran for one hour. The instrument sensitivity was in an acceptable range (see figures 14 and 15), so all of the data from that run was usable.

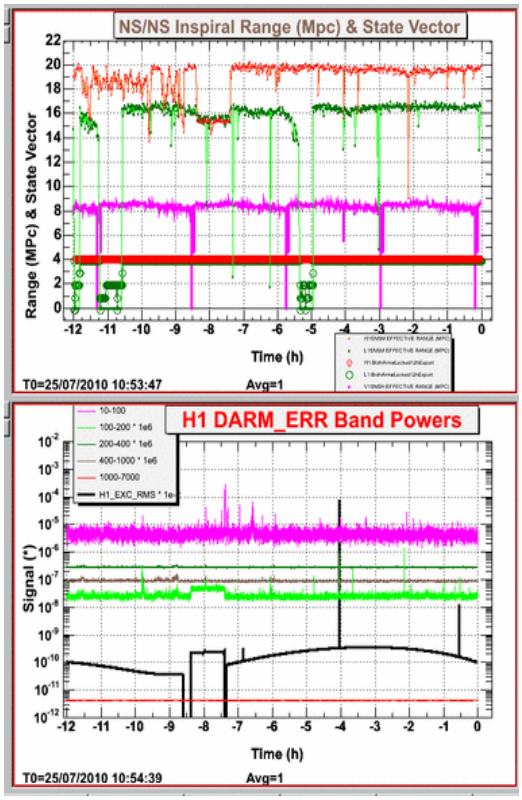

Figure 14: Inspiral range and measured power at WA: second injection. Injection ran from -8.5 to -7.5 hours and both detectors had an inspiral range of about 16 Mpc for the duration of the injection.

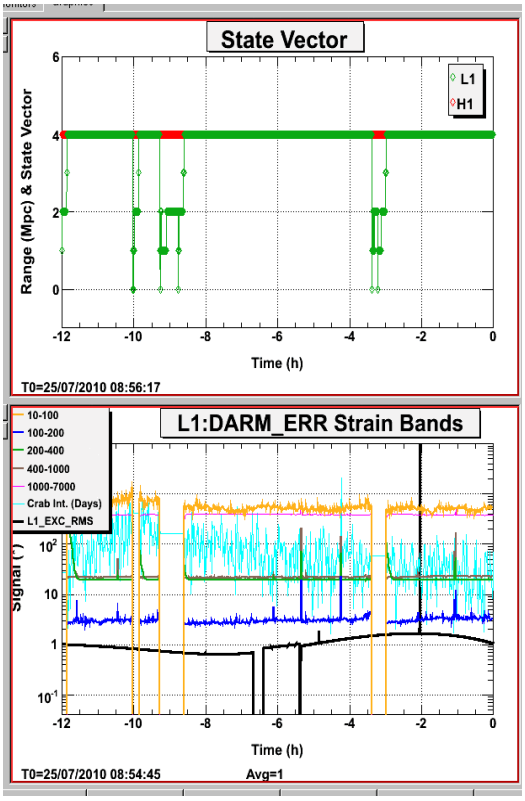

Figure 15: Measured power at LA and state vector: second injection. Injection ran from about -6.5 to -5.5 hours. Explanation of DARM_ERR is in the caption for figure 12. The State Vector shows both detectors operating at their highest sensitivity for the duration of the injection.

II. Recovery

In order to recover the signal from the output data, a recovery code called stochastic.m [10] goes through several data processing steps. The output data from the detectors is a time series and must be transformed to a power spectrum in order to be compared to the original injected signal. Several of the steps for the data processing including high pass filtering, resampling, and frequency masking will be mentioned here [11].

The sampling rate of the detector is about 16kHz, and the greatest sensitivity for the detectors is in the hundred hertz range. In order to suppress the low frequency contributions (below 40 Hz), a high pass filter is applied to the time series, and then the data is resampled which effectively changes the sampling frequency from 16kHz to 1kHz

by averaging several data points. Certain frequencies are masked or rejected from the analysis because there is known instrumental or environmental contamination at these frequencies.

This processed time series is then Fourier transformed to a frequency series, and decomposed into spherical harmonics to be combined as an angular power spectrum. The details of the algorithm can be found in the paper by Thrane *et al*. A basic outline of the process will be addressed here.

The frequency series from the two detectors are combined as shown in

$$C(f,t) \equiv \frac{2}{\tau} \bar{s}_1^*(f) \bar{s}_2(f)$$

where τ is the duration of the analyzed time segments, and $\bar{s}_1^*(f)$ and $\bar{s}_2(f)$ are the strain frequency series from each detector.

It can be shown that [8]

$$\langle C(f,t) \rangle = \sum_{l,m}^{l_{\max}} \bar{H}(f) \gamma_{lm}(f,t) P_{lm}$$

where $\bar{H}(f)$ is the strain power spectrum which we assume to be constant in this analysis, l_{max} is the assumed maximum value of *l* which also defines the angular resolution of the search, $\gamma_{lm}(f,t)$ are the overlap reduction functions, and P_{lm} are the spherical harmonic coefficients. The overlap reduction functions account for the rotation of the earth, the separation and orientation of the detectors, and their sensitivity to locations in the sky.

Using maximum likelihood technique, the P_{lm}'s are estimated from *C(f,t)* and $\gamma_{lm}(f,t)$ functions in order to construct the power distribution

$$P(\Omega) = \sum P_{lm} Y_{lm}$$

The energy density of the source can be found by integrating over the sky distribution

$$\Omega_{gm}(f) \equiv \frac{2\pi^2}{3H_0^2} f^3 \int_{S^2} d\hat{\Omega} P(\hat{\Omega}) \bar{H}(f)$$

where H_0 in the Hubble constant and f is frequency.

Figure 16 shows the sky-distribution of the cross-correlation $P(\Omega)$, as defined above. Figure 17 shows the corresponding uncertainty map. Figure 18 is obtained by dividing the maps in figures 16 and 17 location-by-location.

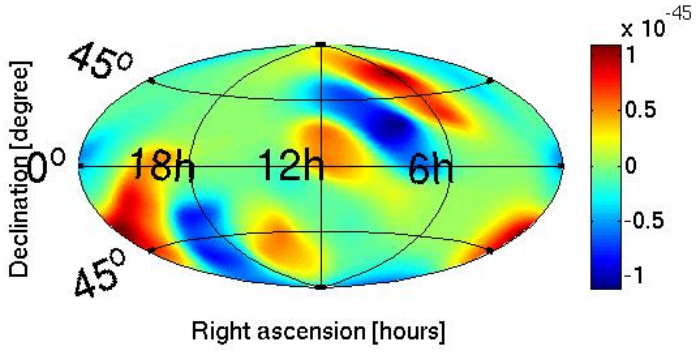

Figure 16: Sky map of cross power. This sky map is the cross power of the two detectors for the three hours of coincidence time. The highest power is 1.1e-45 $strain^2 / Hz / rad^2$ **at 6hr 30minutes, 63 degrees.**

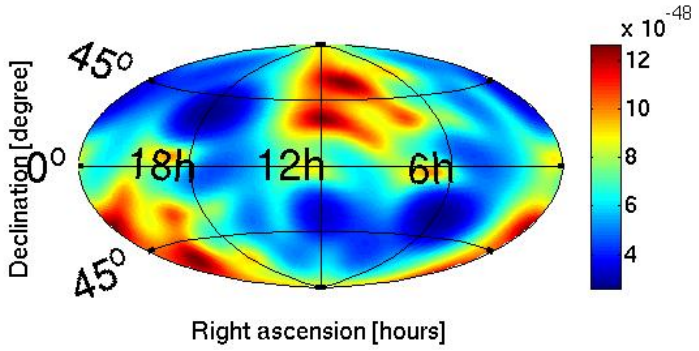

Figure 17: Sky map of statistical uncertainty in measured cross power. The sensitivity at 6hr, 63 degrees was 9e-48 $strain^2 / Hz / rad^2$ **in the same units as cross power.**

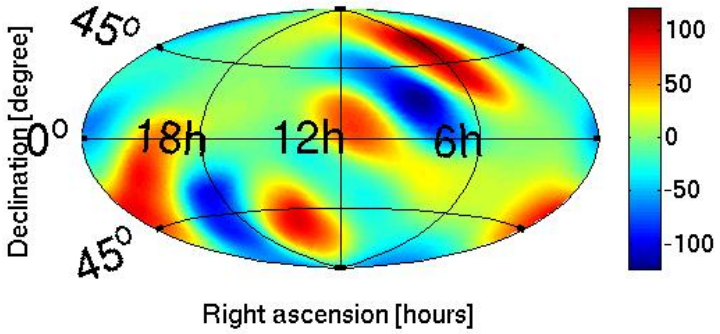

Figure 18: Sky map of Signal to Noise ratio. SNR is determined by dividing the power by the uncertainty in each respective location. The highest value is 119 at 6hr 30minutes, 63 degrees. This sky map plots the ratio of maps in figures 16 and 17.

The highest power in cross power map is 1.1e-45 $strain^2 / Hz / rad^2$ at the location 6 hours 30 minutes, 63 degrees.

The uncertainty in location for declination is determined by

$$\frac{total\_degrees}{l_{max}}$$

and for the right ascension is determined by

$$\frac{total\_degrees\_ra}{m}$$

where the $l_{\max}$ and m values relate to the location resolution of the recovered signal. If the $l_{\max}$ value is increased, the resolution of the location will improve, however, $l_{\max} = 5$ was chosen because there was a recovery code already written for this range of resolution. The value of m ranges from $-l_{\max}$ to $l_{\max}$. The uncertainty in the declination angle is $\pm 36 degrees$ and in the right ascension is $\pm 32.7 degrees$ or $\pm 130 minutes$. The location of the "hot spot" or highest SNR is therefore consistent (within errors) with the intended injection location.

The total uncertainty in the recovered power is the sum of the systematic uncertainty of the instruments and the statistical uncertainty shown in figure 17.

$$\sigma_{total}^2 = \sigma_{statistical}^2 + \sigma_{systematic}^2$$

The systematic uncertainty is dominated by the calibration uncertainties in both detectors, which were estimated to be 5% and 10% for Hanford and Livingston respectively [12]. After adding these is quadrature, the combined systematic error is 11% of the measured power

$$\sigma_{systematic} = P_{meas} \times 0.11$$

giving $\sigma_{systematic} = 1.2 \times 10^{-46}\ strain^2 / Hz / rad^2$. The statistical uncertainty given in the uncertainty sky map in the location of the recovered signal is $\sigma_{statistical} = 9 \times 10^{-48}$ $strain^2 / Hz / rad^2$, which is significantly smaller than the systematic uncertainty. The

total uncertainty in the measurement is then dominated by the systematic uncertainty with a value of $\sigma_{total} = 1.2 \times 10^{-46}\ strain^2 / Hz / rad^2$. The measured power signal is 1.5 standard deviations of the expected power signal (i.e. it is consistent with the expected power)

$$\frac{\left|P'_{theo} - P_{meas}\right|}{\sigma_{tot}} = \frac{\left|0.93 \times 10^{-45}\ strain^2 / Hz / rad^2 - 1.1 \times 10^{-45}\ strain^2 / Hz / rad^2\right|}{1.2 \times 10^{-46}\ strain^2 / Hz / rad^2} = 1.5$$

Chapter 5: Conclusion

I. Overview of project

The purpose of this project was to do a search pipeline test using an anisotropic stochastic signal. This signal was previously implemented by the Stochastic Working Group in software injections. We made the necessary code modifications to perform hardware injections of this signal by physically moving the interferometer mirrors in order to simulate the presence of an anisotropic stochastic gravitational wave background. The injection was intended to run for a 24-hour period, however due to malfunctioning at 1000 minutes of the first run and poor instrument sensitivity it produced a total of three hours of usable data in two separate runs. The recovered power was 1.5 standard deviations away from the expected power. The location of the source also falls within the uncertainty of both location coordinates. The sources of uncertainty include the sensitivity of both detectors at the time of the injection and the calibration constant for transfer functions of the detectors. Improvements that could be made for this injection would be running it either during a lower noise period for the entire 24-hours or

in several hour segments. The results from this pipeline test will be included in the report of the 5th science run for LIGO and provide evidence that the instrument responds to a physical anisotropic stochastic signal as we were expecting. Further work can be done by using other simulated anisotropic stochastic signals from software injections as hardware injections or by injecting the point source signal again with higher resolution.

References

[1] Hulse, R., and J. Taylor. "Discovery of a pulsar in a binary system." *Astrophysical Journal*, no. 195 (1975): L51-L53.

[2] Cuifolini, I., and V. Gorini. "Gravitational waves, theory and experiment (an overview)." In *Gravitational Waves*, edited by I. Cuifolini, Gorini V., U. Moschella and P. Fre, 2-3. Institute of Physics Publishing, 2001.

[3] Lu, J. *et al*. "Detection of gravitational waves." *Reports on Progress in Physics* 63, no. 9 (2000): 1317-1427.

[4] Cyburt, R., B. Fields, K. Olive, and E. Skillman. "New BBN limits on Physics Beyond the Standard Model from He4." *Astroparticle Physics*, no. 23 (2005): 313-323.

[5] Maggiore, M. "Gravitational wave experiments and early universe cosmology." *Physics Reports*, no. 331 (2000): 283-367.

[6] Abbott, B. *et al.* "Detector description and performance for the first coincidence observations between LIGO and GEO." *Nuclear Instruments and Methods in Physics Research Section A* 517 (2004): 154-179.

[7] Abbott, B. *et al*. "An upper limit of the stochastic gravitational-wave background of cosmological origin." *Nature*, no. 460 (2009): 990-994.

[8] Thrane, E. *et al*. "Probing the anisotropies of a stochastic gravitational-wave background using a network of ground-based laser interferometers." 2009.

[9] Kandhasamy, S. "Stochastic gravitational wave search." 2009. Report for Oral exam at the University of Minnesota

[10] Romano, J., J. Whelan, M. McHugh, and V. Mandic. "stochastic.m." [computer program]

[11] Romano, J., and Allen, B. "Companion technical note to the S3 stochastic IFO-IFO analysis paper." 2005.

[12] Mandic, V. 2011. [personal communication]

[13] Abbott, B. *et al*. "Searching for a stochastic background of gravitational waves with the laser interferometer gravitational-wave observatory." *The Astrophysical Journal*, no. 659 (2007): 918-930.

[14] Thrane, E. and Pihlaja, M. 2010